RESEARCH ARTICLE
doi: 10.2306/scienceasia1513-1874.2025.002

ScienceAsia 51 (1): 2025: ID 2025002: **1–6**

Total length distribution in relation to the development of selected organs in marine water-strider *Halobates hayanus* (White, 1883) (Heteroptera, Gerridae)

Pisit Poolprasert[a], **Sinlapachai Senarat**[b], **Nisreen Dahlan**[c], **Koraon Wongkamhaeng**[d], **Natthawut Charoenphon**[e], **Anjaree Inchan**[f], **Narit Thaochan**[g,*]

[a] Department of Entomology, Faculty of Agriculture, Kasetsart University, Bangkok 10900 Thailand
[b] Division of Biological Science, Faculty of Science, Prince of Songkla University, Songkhla 90110 Thailand
[c] Department of Marine Science and Environment, Faculty of Science and Fisheries Technology, Rajamangala University of Technology Srivijaya, Trang Campus, Trang 92150 Thailand
[d] Department of Zoology, Faculty of Science, Kasetsart University, Bangkok 10900 Thailand
[e] Department of Anatomy, Faculty of Medical Science, Naresuan University, Phitsanulok 65000 Thailand
[f] Faculty of Medicine, Praboromarajchanok Institute, Ministry of Public Health, Nonthaburi 11000 Thailand
[g] Agricultural Innovation and Management Division (Pest Management), Faculty of Natural Resources, Prince of Songkla University, Songkhla 90110 Thailand

[*]Corresponding author, e-mail: narrit.t@psu.ac.th

Received 26 Dec 2023, Accepted 14 Oct 2024
Available online 15 Feb 2025

ABSTRACT: The marine water-strider *Halobates hayanus* is prevalent in tropical and subtropical marine habitats. Although the ecology and the morphology of this insect are widely accepted, some histological data remain limited. In this study, we determined new data on the organ histological development for specific performance of *H. hayanus*, locally collected with respect to its total length (TL) from Libong Island, Thailand. Our observation revealed that the TL of this insect could be divided into three groups: (1) Small, 0.1–0.2 cm; (2) Medium, 0.3–0.4 cm; and (3) Large, 0.5–0.6 cm. Histologically, subsequent microscopic development of eyes, Malphigian tubules, midgut, and gonads of *H. hayanus* were found in Group (3), 0.5–0.6 cm in TL. Surprisingly, the distinctive structure of pigment cells, with strong pigment granules and crystalline cones, was also found in the 0.5–0.6 cm group. Clear mature testes with the presence of sperms were evident in the 0.1–0.2 cm group, and the sampled females from the 0.5–0.6 cm group had mature ovaries with the presence of the vitellogenic stage. The results obtained from this study expanded the histological data of *H. hayanus* from natural environments, contributing to further determination of the insect's development stages and physiology.

KEYWORDS: histological features, marine-water strider, reproductive development, selected organs, the *Halobates*

INTRODUCTION

Critical parameters in the distribution of body size influencing community and ecosystem structure in aquatic invertebrates have been reported [1, 2]. Although it is simple to notice how the body size determination can result in significant organization of structure and histological features under the growth performance and the metabolic rate in various invertebrates [2–4], the development process of organs and cells of insects has been limited. A few detailed observations showing the body size was associated with the midgut development and the process of symbiont colonization in the brown-winged green stinkbug *Plautia stali* (Hemiptera: Pentatomidae) [5], and for the larvae and adults of the green lacewing *Chrysoperla externa* (Neuroptera, Chrysopidae) [6]. The larval midgut of *C. externa* appeared as an enlarged sac-like organ and a diverticulum connected with large tracheal trunks in adults.

The marine water-strider *Halobates hayanus*, belonging to the family Gerridae of the order Hemiptera, is an abundant species commonly found in coastal habitats of Thailand as well as other tropical and subtropical marine habitats [7]. *H. hayanus* disperses and colonizes effectively, with passive migration aided by ocean currents and wind allowing it to inhabit a significantly broad geographical range [7–9]. Data from oceanic *H. hayanus* have been published in great taxonomy, phylogenetic systematics, ecology, and zoogeography [10, 11] throughout the metal and lipid composition [11]. While the histological structures of various insects, including their integumentary, nervous, digestive, excretory, and reproductive systems, have been extensively described [12–15], the basic histology of *H. hayanus* has also been comprehensively documented [9]. However, the development of its organs remains largely unexplored. Therefore, the objective of this research was to use histological methods to characterize the organ development of *H. hayanus* during its complete length distribution as a novel insight into academic data to support future observations.

MATERIALS AND METHODS

Thirty active samples of *H. hayanus* were collected from the shallow coastal waters at the Dugong Tourism

by Drones site (7°13′20.6″N 99°24′08.3″E, Libong Island, Thailand. The samples were austerely collected following the recommendations of the Animal Care and Use Committee of Rajamangala University of Technology Srivijaya (Protocol Review No. IAC 13-03-64). The *H. hayanus* individuals were euthanized by rapid cooling shock [16]. The total length (TL) from the head to the tip of abdomen of all samples was measured using a digital vernier caliper (Series: 500–150–30, Mitutoyo, Japan). Then, the specimens were immediately fixed with Davidson's fixative for 24 h at ambient temperature. Their whole bodies were prepared for histological evaluation following the method of Kongthong et al [17]. The paraffin blocks were sectioned at 4 µm thickness in both frontal and longitudinal plans with a rotary microtome and, then, specially stained with PAS (Periodic Acid Schiff) staining protocol to observe the structural organizations including eye, midgut, malphigian tubule, and gonads. All histological slides were visualized and scanned with PANNORAMIC Digital Slide Scanners (3DHISTECH Ltd., Budapest, Hungary).

For morphometric and statistical observations, all investigations including cornea lens lengths (µm), crystalline cone lengths (µm), retinula cell lengths (µm), and midgut epithelium thickness (µm) in the female samples were completed using 30 replicates. Using ImageJ software and with slight modifications of the method described by Reinstein et al [18], we captured digital images at 100x magnification and took measurements at 10 points per field of view (FOV). GraphPad Prism Software Inc. (San Diego, CA, USA) was employed to perform statistical analysis on the raw data to determine significant differences in the results. Multiple comparisons through groups, were performed using a one-way analysis of variance (ANOVA) with Tukey-Kramer post hoc. All results were expressed as mean ± SEM and were considered significant at $p \leqslant 0.05$.

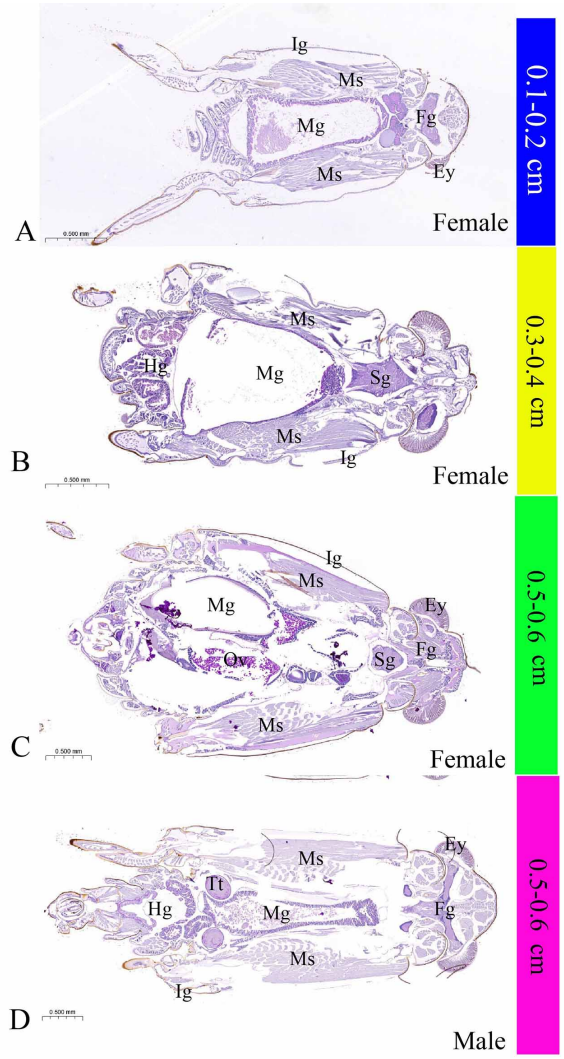

Fig. 1 Overall histological observation in the frontal plans in *H. hayanus* female and male of different total lengths. A, 0.1–0.2 cm female; B, 0.3–0.4 cm female; C, 0.5–0.6 cm female; D, 0.5–0.6 cm male. Abbreviation: Ig, integument; Ms, muscle; Fg, frontal ganglion; Sg, subesorphageal ganglion; Ey, eye; Mg, midgut; Hg, hindgut; Ov, ovary; and Ts, testis.

RESULTS AND DISCUSSION

Overall histology

The *H. hayanus* samples were categorized into three groups based on total length (TL, from head to tip of abdomen): small, S (0.1–0.2 cm, $n = 5$ female); medium, M (0.3–0.4 cm, $n = 5$ female); and large, L (0.5–0.6 cm, $n = 7$ male and $n = 13$ female). Fig. 1 shows that all groups shared histological characteristics. As noted in *H. hayanus* [9], the examined organs included the integument, muscle, frontal ganglia, subesophageal ganglion, eye, midgut, hindgut, and gonads (ovary and testis).

Eye development

The frontal sections of the paired compound eyes of the apposition (photopic) type of *H. hayanus* in all groups displayed comparable patterns (Fig. 2). Several ommatidia from the 0.1–0.2 cm TL group showed closely packed hexagonal facets, with each ommatidium having a regular and elongated shape (Fig. 2A). Each ommatidium was divided into two distinct zones, outer and inner, and possessed a transparent bi-convex lens with a slight pinkness in the cytoplasm of the eye in the outer zone (Fig. 2B). Multiple cell types were detected in the inner zone, including crystalline cone, primary pigment cell with few pigment granules, and photoreceptor cell (or retinular cell) (Fig. 2C), which were also found from the 0.3–0.4 cm TL group (Fig. 2C,D). Meanwhile, well-developed crystalline cones and pri-

Table 1 Morphometric parameters (corneal lens length, crystalline cone length, retinula cell length, muscle area, and epithelium thickness) of female *H. hayanus* at different body sizes.

Parameter	Size of female		
	$n = 5$	$n = 5$	$n = 7$
	0.1–0.2 cm	0.3–0.4 cm	0.5–0.6 cm
Cornea lens lengths (μm)	6.17 ± 0.18^{a}	10.67 ± 0.30^{b}	19.91 ± 0.23^{c}
Crystalline cone lengths (μm)	27.88 ± 0.89^{a}	28.43 ± 0.40^{a}	39.36 ± 0.73^{b}
Retinula cell lengths (μm)	101.15 ± 3.49^{a}	111.42 ± 3.18^{b}	122.02 ± 1.58^{c}
Midgut epithelium thickness (μm)	8.63 ± 0.09^{c}	8.19 ± 0.10^{b}	5.61 ± 0.06^{a}

Data are expressed as mean ± SEM. Different letters (a, b, c) indicate significant differences ($p < 0.05$) between groups based on post-hoc tests following one-way ANOVA.

mary pigment cells with noticeable brown-pigment granules were discovered from the 0.5–0.6 cm TL group and within the ommatidium (Fig. 2E,F). However, the TL of the insect was positively correlated to several parameters ($p \leqslant 0.05$), as shown in Table 1, namely cornea lens lengths, crystalline cone lengths, retinula cell lengths, and muscle areas. These results were consistent with previous reports from many insect groups such as butterflies, bees, ants, and beetles, etc. Retinula cells create all insect visual pigments and stored them in the rhabdoms (Rhabmomeres) of the compound eyes and the ocelli (simple eyes), and the rhabdoms are linked to the optic lobe of protecerebrum, with a key role for absorbing color and ultraviolet (UV) light. It demonstrated that *H. hayanus* had an extensive field of eye function. Additionally, size and arrangement of ommatidia in the compound eyes could be influenced by body size, as reported by a prior review [19–23]. Common pigments containing photostable pigment granules, which include ommochromes and pteridines [24, 25], might block an off-axis light, a prerequisite to separate visual inputs of neighboring photoreceptors [26]. Furthermore, insect muscle tissue was positively correlated with metamorphosis, with most larval muscles histolyzed during metamorphosis and replaced by adult muscles generated from adult muscle founder cells [27, 28]. The finding could be used to support physiological observations of insect eyes and muscles in future investigations.

Malphigian tubule development

The arrangement patterns of malphigian tubules (MTs) in all groups were identical (Fig. 3A,B), but the cell size with the prominent apical surface was a driving observation (Fig. 3B). MTs were lined with simple cuboidal epithelial cells that could be spotted at the midgut , similar to those found in the other marine waterstrider, *Asclepios annandalei* [29]. Tubule size were 98.3 ± 0.5 μm, 112.4 ± 0.76 μm, and 125 ± 0.67 μm in the S, M and L groups, respectively. It was suggested that the increase of the tubule size was due to the increased functions of the main excretory organs, including mucopolysaccharides and protein syntheses, dietary waste, and a range of nitrogenous materials [30]. Furthermore, it was hypothesized that the physiological requirement of insects might boost the excretory load of MTs because insects grow through consecutive larval instars. As a result, insect MTs evolve in a couple of ways, such as enlargement by cell proliferation of a few tubules (formed early in embryogenesis) or the formation of additional tubules in accordance with the instar number. Consequently, adult insects have more tubules than those at juvenile stages. If there are more than 200 tubules; however, the tubules are alternatively small [31]. It has been proposed that MTs can be employed for assessing biomarkers, detoxification, and innate immunity, as well as models for human kidney diseases [32]. As a result, it could be useful for multiple purposes in insect physiology as well as therapeutic treatment in other vertebrates.

Midgut epithelium development

Several cell types in the midgut epithelium were described and grouped into three cell types (types I, II, and III), which were the first observation in *H. hayanus* (Fig. 3C–E). Type I cells possessed cuboidal cells, and their cytoplasm was characteristically spongy-like due to the abundance of unstained vacuoles (Fig. 3C). The type II cells were similarly found as the previous cell type, but the rare unstained vacuoles were also visible (Fig. 3C,D). The rare type III cells had a triangular shape and an oval nucleus close to the cell base (Fig. 3C). These findings were in accordance with those previously reported [33, 34]. We suggested that type I and type II cells might be secretory cells containing secretory granules. The midgut epithelium of *H. hayanus* may be involved in producing digestive enzymes that play important roles in digestion, absorption, secretion, and cell regeneration [35]. The apical surface, positively stained with PAS (Fig. 3D,E), was rarely observed in the L group (Fig. 3E), whose epithelial layer was well-lined with a peritrophic membrane. In addition, the thickness of the midgut epithelium decreased and was substantially thinner in the adult stage ($p \leqslant 0.05$), as demonstrated in Table 1. In this case, midgut epithelium might degenerate before each molting till adulthood [36]. The degeneration

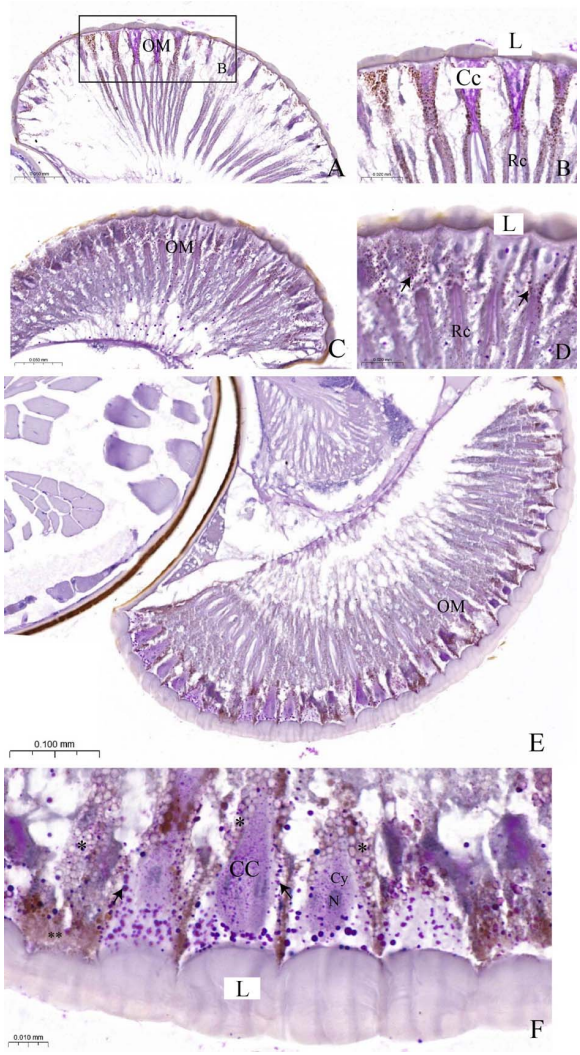

Fig. 2 Light microscope observation of eye structure in *H. hayanus* of different total lengths. A–B, 0.1–0.2 cm; C–D, 0.3–0.4 cm; and E–F, 0.5–0.6 cm. Elongated shape of ommatidia is covered the Len (L) and each contained the crystalline cone (CC), primary pigment cell (arrows) with the brown-pigment granules (asterisks) and retinula cells (Rc). The brown-pigment granules (arrows)

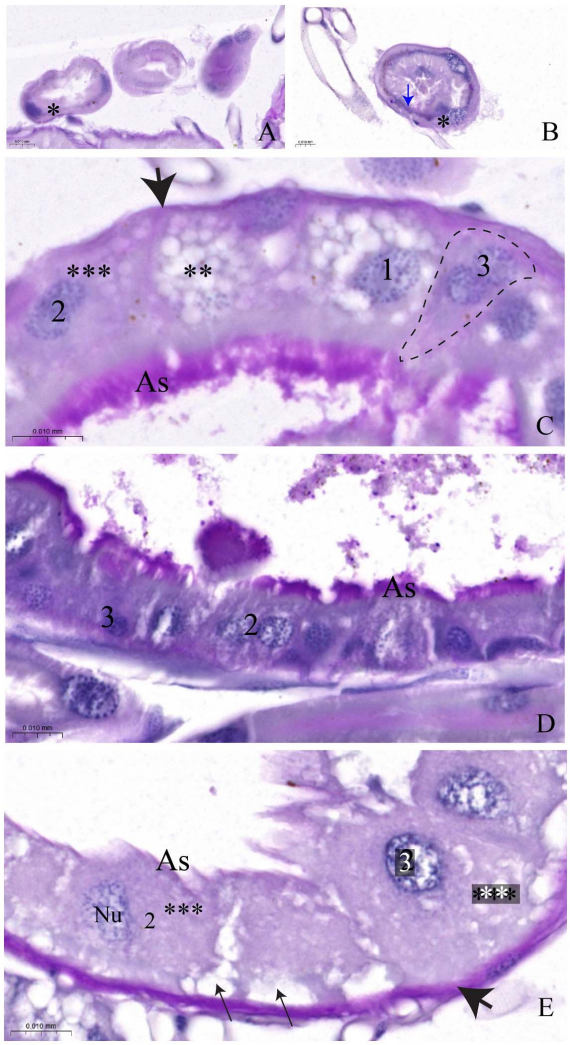

Fig. 3 Light microscope observation of malphigian tubule (A–B) and midgut (C–E) in *H. hayanus* of different total lengths: A, 0.1–0.2 cm; B–D, 0.3–0.4 cm; and B,E, 0.5–0.6 cm. In A, a small size of Malpighian tubules (asterisk) was found, when compared with the large size (asterisk). Midgut epithelium is composed of three cell types (type 1, 2, and 3) each with different features. Abbreviations: As, apical surface; **, foamy accumulation; Large arrows, peritoneal membrane; and small arrow, artifacts.

referred to as apoptosis, autophagy, or necrosis, and it was vital to maintain homeostasis by disintegrating the organelles using vacuoles and/or lysosomes found in both vertebrates and invertebrates [37, 38]. Autophagy has been observed in the midgut epithelium of the house cricket (*Acheta domesticus*), where phagophores encase cytoplasm and organelles like mitochondria, forming autophagosomes that gradually degrade these components. Similarly, in marine insects, the stomodeal valve at the esophagus's end in the metathorax separates the foregut from the midgut. This valve, formed by the invagination of the esophagus, is associated with Cuénot cells, which may rupture due to pollutants or environmental changes. In salt marsh chironomids (Chironomidae), such cell rupture often indicates physiological stress or damage from environmental contamination [39].

Gonadal development

Senarat et al [9] reported paired testes in *H. hayanus*, which are also observed in other gerrids like *Gerris lacustris* [40]. In the S group, the testicular folli-

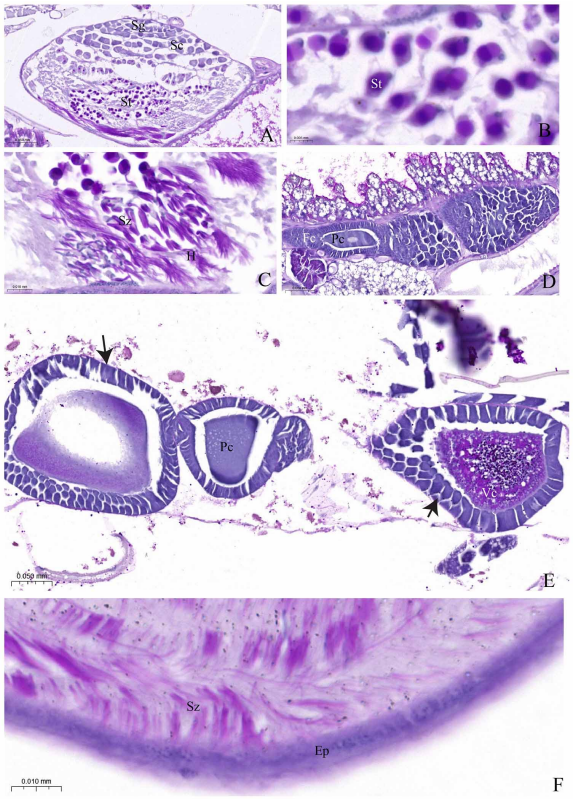

Fig. 4 Light microscope observation of male and female gonad development in *H. hayanus* of different total lengths: A–C, 0.1–0.2 cm; D, 0.3–0.4 cm; and E–F, 0.5–0.6 cm. Abbreviations: Ep, epithelial layer; H, head; Pc, previtellogenic stage; Sg, spermatogonia;, Sc, spermatocyte; St, spermatids; Sz, spermatozoa; Vc, vitellogenic stage; arrows, follicle cell.

cle contained the spermatogonia, spermatocytes, and spermatids (Fig. 4A). The spermatid showed an oval shape, basophilic nucleus, and slightly basophilic cytoplasm (Fig. 4B). Interestingly, the development of tail formation at this stage was noted in Fig. 4B and the development of rare spermatozoa in Fig. 4C. The previtellogenic stage close to the nurse cell was identified in the M group (Fig. 4D). When compared with the L group, the sampled species showed the vitellogenic stage with the prominent yolk granules (Fig. 4E) and the observed spermatozoa with association to the epithelial layer (Fig. 4F).

This study also showed that the development of male spermatozoa began at 0.1–0.2 cm TL, whereas female entered the vitellogenic stage when the TL reaching 0.5–0.6 cm, indicating that the males of *H. hayanus* matured more rapidly than the females.

CONCLUSION

Organ development in *H. hayanus* from Libong Island showing well-developed structures started in the 0.5–0.6 cm TL group. It is noted that the males, with their visible spermatozoa, exhibited faster development than the females, whose reproductive structures were less developed at the same stage. These findings are significant for understanding the development and the physiology of *H. hayanus*.

Acknowledgements: The sample preparation has been completed in the Faculty of Science and Fisheries Technologgy, Rajamangala University of Technology Srivijaya Trang Campus. The processes have been totally completed in the Microtenique Laboratory, Division of Biological Science, Faculty of Science, Prince of Songkla University and the Department of Anatomy, Faculty of Medical Science, Naresuan University, Thailand.

REFERENCES

1. Schmidt-Nielsen K (1984) *Scaling: Why Is Animal Size So Important?* Cambridge Univ Press, UK.
2. Bourassa N, Morin A (1995) Relationships between size structure of invertebrate assemblages and trophy and substrate composition in streams. *J North Am Benthol Soc* **14**, 393–403.
3. Hanken J, Wake DB (1993) Miniaturization of body size: organismal consequences and evolutionary significance. *Annu Rev Ecol Syst* **24**, 501–519.
4. Yamanaka T, White PC, Spencer M, Raffaelli D (2012) Patterns and processes in abundance-body size relationships for marine benthic invertebrates. *J Ani Ecol* **81**, 463–471.
5. Oishi S, Moriyama M, Koga R, Fukatsu T (2019) Morphogenesis and development of midgut symbiotic organ of the stinkbug *Plautia stali* (Hemiptera: Pentatomidae). *Zool Lett* **5**, 16.
6. Dantas PC, Serrão JE, Santos HCP, Carvalho GA (2021) Anatomy and histology of the alimentary canal of larvae and adults of *Chrysoperla externa* (Hagen, 1861) (Neuroptera: Chrysopidae). *Arthropod Struct Dev* **60**, 101000.
7. Cheng L (1985) Biology of *Halobates* (Heteroptera: Gerridae). *Annu Rev Entomol* **30**, 111–135.
8. Cheng L, Mishra H (2022) Why did only one genus of insects, *Halobates*, take to the high seas? *PLoS Biol* **20**, e3001570.
9. Senarat S, Saeluea N, Mongkolchaichana E, Charoenphon N, Sittichaya W, Thaochan N, Poolprasert P, Kenthao A, et al (2023) Systemic histology of the marine water-strider *Halobates hayanus* (Heteroptera, Gerridae). *Sains Malays* **52**, 2485–2498.
10. Andersen NM, Cheng L (2004) The marine insect *Halobates* (Heteroptera: Gerridae): biology, adaptations, distribution, and phylogeny. *Oceanogr Mar Biol* **42**, 119–180.
11. Nichols PD, Johns RB (1983) The metal and lipid composition of the sea skaters *Halobates hayanus* (from Australian waters) and *Rheumatobates aestuarius* (from Baja, CA). *Comp Biochem Physiol* **75**, 617–623.
12. Barbosa P, Berry DL, Kary CS (2015) *Insect Histology: Practical Laboratory Techniques*, John Wiley & Sons.
13. Boonyoung P, Senarat S, Kettratad J, Jiraungkoorskul W, Thaochan N, Sing K-W, Pengsakul T, Poolprasert P (2020) Mature gonadal histology and gametogenesis

of the tortoise beetle *Aspidimorpha sanctaecrucis* (Fabricius, 1792) (Coleoptera: Cassidinae: Chrysomelidae): Histological observation. *Songklanakarin J Sci Technol* **42**, 871–878.
14. Somala N, Senarat S, Para C, Jiraungkoorskul W, Kaneko G, Poonpet T, Poolprasert P (2020) Systemic organization of *Tetraponera rufonigra* Jerdon, 1851 (Hymenoptera: Formicidae): Hitological observation. *Serangga* **25**, 53–67.
15. Poolprasert P, Senarat S, Thongboon L, Thaochan N, Mongkolchaichana E, Sukparangsi W, Charoenphon N (2023) Histological organization of tephritid fruit flies (Diptera, Tephritidae) from Thailand. *Songklanakarin J Sci Technol* **45**, 348–355.
16. Wilson JM, Bunte RM, Carty A (2009) Evaluation of rapid cooling and tricaine methanesulfonate (MS222) as methods of euthanasia in zebrafish (*Danio rerio*). *J Am Assoc Lab Anim Sci* **48**, 785–789.
17. Kongthong K, Charoenphon N, Thaochan N, Boonyoung P, Iida A, Jeamah A, Imsonpang S, Wongkamhaeng K, et al (2023) A histological method for marine invertebrates. *Vet Integr Sci* **21**, 251–263.
18. Reinstein DZ, Archer TJ, Gobbe M (2009) Corneal epithelial thickness profile in the diagnosis of keratoconus. *J Refract Surg* **25**, 604–610.
19. Hunt ER, Dornan C, Sendova-Franks AB, Franks NR (2018) Asymmetric ommatidia count and behavioural lateralization in the ant *Temnothorax albipennis*. *Sci Rep* **8**, 5825.
20. Wen C, Ma T, Deng Y, Liu C, Liang S, Wen J, Wang C, Wen X (2020) Morphological and optical features of the apposition compound eye of *Monochamus alternatus* Hope (Coleoptera: Cerambycidae). *Micron* **128**, 102769.
21. Wen C, Pan Z, Liang S, Shen L, Wen X, Wang C (2022) Fine structure of the visual system of *Arge similis* (Hymenoptera, Argidae). *Insects* **13**, 152.
22. Hao Y, Wang Q, Wen C, Wen J (2023) Comparison of fine structure of the compound eyes in *Eucryptorrhynchus scrobiculatus* and *Eucryptorrhynchus brandti* adults. *Insects* **14**, 699.
23. Bankar TN, Dar MA, Pandit RS (2018) Diversity and functions of chromophores in insects: A review. In: Shah MM, Sharif U (eds) *Insect Science-Diversity, Conservation and Nutrition*, IntechOpen, pp 3–18.
24. Vargas-Lowman A, Armisen D, Burguez Floriano CF, da Rocha Silva Cordeiro I, Viala S, Bouchet M, Bernard M, Le Bouquin A, et al (2019) Cooption of the pteridine biosynthesis pathway underlies the diversification of embryonic colors in water striders. *Proc Natl Acad Sci USA* **116**, 19046–19054.
25. Mohr T, Meinertzhagen IA, Fischer S (2020) Novel type of sub-retinal pigment shield in the miniaturized compound eye of *Trichogramma evanescens*. *J Comp Neurol* **528**, 167–174.
26. Gribakin FG, Ukhanov KY (1993) Light scattering in the eye of the blowfly chalky mutant: The effect on spectral sensitivity of photoreceptors R1-6. *Vision Res* **33**, 1185–1191.
27. Gunage RD, Dhanyasi N, Reichert H, VijayRaghavan K (2017) Drosophila adult muscle development and regeneration. *Semin Cell Dev Biol* **72**, 56–66.
28. Bretscher H, O'Connor MB (2020) The role of muscle in insect energy homeostasis. *Front Physiol* **11**, 580687.
29. Poolprasert P, Senarat S, Kettratad J, Kaneko G, Mongkolchaichana E, Charoenphon N, Thaochan T (2022) Comprehensive structure of the female marine water-strider *Asclepios annandalei* Distant, 1915 from Pranburi River estuary, Thailand: New information for the genus *Asclepios*. *Trop Life Sci Res* **33**, 47–60.
30. Farina P, Bedini S, Conti B (2022) Multiple functions of Malpighian tubules in insects: A review. *Insects* **13**, 1001.
31. Nation JL (2022) *Insect Physiology and Biochemistry*, 4th edn, CRC Press.
32. Nocelli RC, Cintra-Socolowski P, Roat TC, Silva-Zacarin EC, Malaspina O (2016) Comparative physiology of Malpighian tubules: form and function. *Open Access Insect Physio* **6**, 13–23.
33. Dai L, Yang B, Wang J, Zhang Z, Yang R, Zhang T, Ren Z, Lin C (2019) The anatomy and ultrastructure of the digestive tract and salivary glands of *Hishimonus lamellatus* (Hemiptera: Cicadellidae). *J Insect Sci* **19**, 3.
34. Fialho MDCQ, Zanuncio JC, Neves CA, Ramalho FS, Serrão JE (2009) Ultrastructure of the digestive cells in the Midgut of the predator *Brontocoris tabidus* (Heteroptera: Pentatomidae) after different feeding periods on prey and plants. *Ann Entomol Soc Am* **102**, 119–127.
35. Terra WR, Ferreira C (2012) Biochemistry and molecular biology of digestion. In: Gilbert LI (ed), *Insect Molecular Biology and Biochemistry*, Vol 1, Academic Press-Elsevier, pp 365–418.
36. Rost-Roszkowska MM, Świątek P, Poprawa I, Rupik W, Swadźba E, Kszuk-Jendrysik M (2015) Ultrastructural analysis of apoptosis and autophagy in the midgut epithelium of *Piscicola geometra* (Annelida, Hirudinida) after blood feeding. *Protoplasma* **252**, 1387–1396.
37. Rost-Roszkowska MM, Janelt K, Poprawa I (2018) The role of autophagy in the midgut epithelium of Parachela (Tardigrada). *Zoomorphol* **137**, 501–509.
38. Muita BK, Baxter SW (2023) Temporal exposure to Bt insecticide causes oxidative stress in larval midgut tissue. *Toxins* **15**, 323.
39. Grueso-Gilaberth RN, Jaramillo-Timarán KS, Ospina-Pérez EM, Richardi VS, Ossa-López PA, Rivera-Páez FA (2020) Histological description and histopathology in *Polypedilum* sp. (Diptera: Chironomidae): A potential biomarker for the impact of mining on tributaries. *Ann Entomol Soc Am* **113**, 359–372.
40. Candan S, Özyurt Koçakoğlu N, Suludere Z (2018) Morphological and histological structure of the male reproductive system of the water strider *Gerris lacustris* (Linnaeus 1758) (Gerridae, Heteroptera). *Microsc Res Tech* **81**, 770–780.